Dynamics of cytoskeletal filaments

Yuri M. Sirenko
Department of Electrical and Computer Engineering, North Carolina State University, Raleigh, North Carolina 27695-7911

Michael A. Stroscio
U.S. Army Research Office, P.O. Box 12211, Research Triangle Park, North Carolina 27709-2211

K. W. Kim
Department of Electrical and Computer Engineering, North Carolina State University, Raleigh, North Carolina 27695-7911

(Received 16 February 1996)

We apply elasticity theory formalism to study long-range, collective vibrations of actin and intermediate filaments, which are long cylindrical macromolecules and constitute part of the cytoskeleton network in eukariotic cells. The dispersion relations are obtained for elastic waves propagating in the vicinity of filaments which are modeled as elastic cylindrical rods immersed in a liquid. In the long-wavelength limit the filament-water system supports two acoustic modes with propagation speeds of approximately 800 and 1300 m/s and a single flexural wave with parabolic dispersion law. The presence of solvent leads to radiation of acoustic energy from waves with a phase velocity exceeding the speed of sound of water. Our study complements the existing normal-mode analysis of free actin filament vibrations and generalizes these results for different structures as well as including the effects of solvents. [S1063-651X(96)12208-X]

PACS number(s): 87.15.−v

I. INTRODUCTION

As evidenced by recent publications [1–3], there is a rising interest in the physical science community in the mechanical properties of cytoskeleton. Besides its own importance, the cytoskeleton components (microtubules and filaments) serve as biological counterparts to recently fabricated nanotubules [4] and free-standing filaments [5]. The cytoskeleton filamentous network, which is found in all eukariotic cells, defines the cell shape and serves as a global framework for mechanical and functional integration of the whole cell [6]. Besides its shape-supporting function, the filament system takes part in chromosomal movement, cell motility [7], provides tracks for guiding transport of particles [8], and could possibly directly transmit signals along the filaments [9].

The components of the cytoskeleton are classified according to their diameter into three major classes [9]: actin filaments (6–10 nm), intermediate filaments (7–11 nm), and microtubules (25 nm). While the microtubules (MTs) have the form of hollow cylindrical *shells* [10], the actin filaments (AFs) and intermediate filaments (IFs) could be in the first approximation modeled as long cylindrical *rods*. More specifically, the results of x-ray fiber diffraction data [11] allow us to describe the AF (F-actin) structure as two-stranded helix consisting of the globular actin (G-actin) monomers. The various types of IFs (including neurofilaments) are formed by several 2–3 nm diameter protofilaments, twisted together like the strands of a rope [9,12].

In a series of experiments, the flexural rigidity and elastic Young's modulus for MTs [13] and AFs [14] have been obtained from the measurement of thermal fluctuations in end-to-end distance of the proteins. In more recent works, the elastic parameters of the cytoskeleton components were determined using Fourier-analysis of thermal fluctuations in shape [15], hydrodynamic flow [16], and direct measurements [17,18].

In this paper we apply the formalism of classical elasticity theory to describe the vibrational modes and mechanical wave propagation in rodlike cytoskeleton components, such as AFs and IFs, immersed in water. This study complements our recent treatment [19] of elastic vibrations in MT-solvent system. This investigation arises in the context of the general problem of protein dynamics [20] and connection between protein dynamics and function [21], as well as the recent advancements in experimental techniques, which enable us to observe directly the movement of a single filament (see, e.g., [18,22]). From the point of view of physiology, the motion of AFs is directly related to such important processes as cell movement [7] and muscle contraction [23]. Analysis of the sliding motion of cytoskeletal filaments, which are propelled by the motor proteins such as myosin and kinesin [2,3,24], allows for better understanding of how a directional motion is created in a Brownian physical system [25]. Recently, the *in vitro* setup, in which the head of AF was spatially fixed, was used to study the symmetry breaking instabilities in spontaneous oscillations of the filament [1]. Finally, our treatment of filament dynamics parallels the ongoing research on acoustic phonon confinement in free-standing [26,27] and buried [28] semiconductor quantum wires.

The simplest possible description of filament and MT vibrations is based on a linear model and is used extensively for analysis of fluctuations in shape [15–17]. Further elaborations of the one-dimensional model have addressed the problem of instabilities in vibrations of AFs [1,3] and soliton propagation in MTs [29] due to inclusion of nonlinear terms in Hamiltonian and polarization effects [30]. The linear model also serves as a basis for theoretical study of elastic properties of cytoskeleton network [31]. Despite the univer-

sality and simplicity of the linear model, its applicability is restricted to a limit of extremely large wavelengths of the propagating waves, where all the diversity of the vibrational spectrum is reduced to pure longitudinal, torsional, and bending modes.

On the other hand, the most exhaustive information about internal motion of all constituent elements of the protein can be obtained from microscopic calculations, such as normal mode analysis [32,33]. In particular, Tirion and ben-Avraham [34] used the a G-actin model [35] to obtain the vibrational spectrum of a G-actin monomer bound with ADP and Ca^{2+}. These calculations required solution of a generalized eigenvalue equation for 1384 torsional degrees of freedom of a 375-residue polypeptide chain. Assigning a thermal energy of $k_BT/2$ (where T is the absolute temperature and k_B is Boltzmann's constant) to each mode, the authors have calculated the average fluctuations in the positions of α-carbon atoms in the chain. It was found that over 50% of the overall motion can be described by first four, slow modes. Later [36], the calculated slow normal modes of G-actin were used as structural parameters to refine the F-actin model [11] against 8-Å resolution x-ray fiber diffraction data.

Most recently, ben-Avraham and Tirion [37] considered propagation of elastic waves in long AFs. Ignoring the internal motion in actin monomers and allowing for quasiperiodicity (helicity) of the F-actin structure, the authors obtained six vibrational branches, corresponding to three translational and three rotational degrees of freedom for each actin monomer. The model describes the binding between actin monomers with the help of a single phenomenological strength constant, which is obtained by fitting to available experimental data. The calculated dependence of mode frequency ω on the wave phase ϕ reproduces qualitatively the results of the linear model, and also describes the internal motion of AF.

Though the normal mode analysis, based on the solution of equations of motion for all microscopic degrees of freedom, provides detailed information on both large-scale and local conformal motion, it lacks some attractive features of the linear model, such as universality and simplicity. Each protein configuration requires separate *ad hoc* calculations, which become rather cumbersome with the increase in protein size. Besides, the detailed information on each vibrational mode is often not required, since many fundamental features of conformal motion can be explained using only the slowest, large-scale collective vibrations. Finally, the inclusion of solvent effects into the microscopic calculations is not straightforward, especially under conditions when there is radiation of acoustic energy from the vibrating protein into the surrounding water. Description of such processes requires consideration of large volumes of the solvent, which therefore cannot be treated microscopically, but rather as a continuous medium.

In this paper we extend the applicability of a simple linear model, by taking into account the internal motion of proteins by treating the interior as a continuous medium. Application of a standard formalism of elasticity theory [38] allows the description of universal features of wave propagation in arbitrary cylindrical and hollow protein filaments. Such a treatment complements the normal mode analysis, which requires *ad hoc* calculations tailored to a specific structure [37] and revealing both universal and microscopic, model-specific details of the vibrational spectrum. Universal properties of long protein dynamics are also of major importance to many protein functions, since they represent long-range, slow, collective conformal motions of the protein.

Microscopic and elastic-medium approaches also complement each other in a sense that they have different (though overlapping) ranges of applicability. The microscopic calculations work best for systems with small numbers of constituent elements, such as AFs. To the contrary, with the increase of the filament diameter (IFs and MTs), the accuracy and limits of applicability of the continuous-medium formalism increase, while the amount of computations and number of required fitting parameters for the microscopic calculations grow significantly. An additional benefit of the macroscopic treatment is that it makes possible the inclusion of the effects of the surrounding solvent in a natural and simple way [39]. Macroscopic consideration of vibrations in a water-protein system provides insight into the effects of solvent on protein dynamics, and could facilitate the introduction of reasonable physical approximations to be used in microscopic calculations.

The rest of the paper is organized as follows. In Sec. II we derive the general dispersion relations for waves supported by a filament-fluid system; the analysis of the vibrational spectrum follows in Sec. III, while the numerical results and discussion are provided in Sec. IV. Finally, Sec. V contains conclusions, and the Appendix details properties of Bessel's functions used in the text.

II. BASIC EQUATIONS

We model filaments (IFs and AFs) with an infinitely long elastic cylinder immersed in water and occupying the region $r<R$. The material of the cylinder is assumed to be isotropic with Young's modulus E and Poisson's ratio ν, and density ρ. Below we apply the standard formalism of classical elasticity theory, thus ignoring the solvent viscosity and the friction between the water and filament.

The general solution of the elasticity equations for displacement vector $\mathbf{u}$ inside the cylinder ($r<R$) can be written in the form [38]

$$\mathbf{u}=\nabla\phi+\nabla\times(\mathbf{e}_z\psi)+R\nabla\times\nabla\times(\mathbf{e}_z\chi). \tag{1}$$

Here $\mathbf{e}_z$ is a unit vector along the axis z, and potential(s) ϕ (ψ, χ) satisfy scalar wave equation with a propagation speed equal to longitudinal (transverse) sound speed s_l (s_t) in cylinder material, where

$$s_l^2=\frac{1-\nu}{(1-2\nu)(1+\nu)}\,\frac{E}{\rho},\quad s_t^2=\frac{E}{2(1+\nu)\rho}.$$

For the outer region, $r>R$, the displacements of water $\mathbf{u}_w$ is specified by a scalar potential Φ:

$$\mathbf{u}_w=\mathrm{grad}\,\Phi. \tag{2}$$

In order to describe harmonic vibrations (with frequency ω and wave vector $k_z\equiv k/R$) in a coupled cylinder-water system, localized near the surface of the filament, we set

$$\left.\begin{matrix}\Phi\\ \phi\\ \psi\\ \chi\end{matrix}\right\}=\frac{1}{R}\times\left\{\begin{matrix}ic_0K_m(\kappa_w r/R)\\ ic_1I_m(\kappa_l r/R)\\ c_2I_m(\kappa_t r/R)\\ c_3I_m(\kappa_t r/R)\end{matrix}\right\}\times\exp(im\varphi+ikz/R-i\omega t). \tag{3}$$

In writing Eq. (3), it is assumed that the quantities (s_w is a sound speed in water)

$$\kappa_t^2=k^2-(\omega R/s_t)^2,$$

$$\kappa_l^2=k^2-(\omega R/s_l)^2,$$

$$\kappa_w^2=k^2-(\omega R/s_w)^2$$

are positive. Note that in the opposite case of $\kappa_w^2<0$ (i.e., $\omega>s_w k_z$) the acoustic energy is radiated from the filament into surrounding water. Also, if $\kappa_{l,t}^2<0$, the corresponding scalar potentials specify *confined* vibrations, which do not decay exponentially towards the center of the filament. The vibrations with negative κ_w^2, κ_l^2, or κ_t^2 can be still treated with the help of Eq. (3) using analytical properties of Bessel's functions, as shown in the Appendix.

Substituting the potentials ϕ, ψ, and χ from Eq. (3) to Eq. (1), we find the components of the displacement vector in the filament,

$$\begin{aligned}-iu_r(r)&=\kappa_l c_1 I_m'(\kappa_l r/R)+mc_2(R/r)I_m(\kappa_t r/R)\\&\quad+k\kappa_t c_3 I_m'(\kappa_t r/R),\\-u_\varphi(r)&=mc_1(R/r)I_m(\kappa_l r/R)+\kappa_t c_2 I_m'(\kappa_t r/R)\\&\quad+mkc_3(R/r)I_m(\kappa_t r/R),\\-u_z(r)&=kc_1 I_m(\kappa_l r/R)+\kappa_t^2 c_3 I_m(\kappa_t r/R).\end{aligned} \tag{4}$$

From continuity of the displacements of water and filament at $r=R$ we obtain

$$c_0=\frac{1}{\kappa K_m'(\kappa)}[\kappa_l c_1 I_m'(\kappa_l)+mc_2 I_m(\kappa_t)+k\kappa_t c_3 I_m'(\kappa_t)].$$

Applying standard boundary conditions [38] for a stress tensor at $r=R$, and expressing the water pressure p in terms of scalar potential,

$$p=-\rho_w\ddot{\Phi}, \tag{5}$$

where ρ_w is a water density, we arrive at the eigenequation for elastic vibrations of coupled water-filament system:

$$\mathcal{D}[c_1,c_2,c_3]^{\mathbf{T}}=0\,, \tag{6}$$

where the matrix $\mathcal{D}$ is equal to

$$\mathcal{D}=\begin{bmatrix}2m(I_{l0}-I_{l1}) & -(\kappa_t^2+2m^2)I_{t0}+2I_{t1} & 2mk(I_{t0}-I_{t1})\\ -2kI_{l1} & -mkI_{t0} & -(\kappa_t^2+k^2)I_{t1}\\ (2m^2+k^2+\kappa_t^2)I_{l0}-2(1+W)I_{l1} & 2m[I_{t1}-(1+W)I_{t0}] & 2k[(m^2+\kappa_t^2)I_{t0}-(1+W)I_{t1}]\end{bmatrix}. \tag{7}$$

Here we use notations $I_{l,t0}\equiv I_m(\kappa_{l,t})$ and $I_{l,t1}\equiv\kappa_{l,t}I_m'(\kappa_{l,t})$; the term

$$W\equiv\frac{\rho_w}{\rho}\,\frac{K_m(\kappa_w)}{-2\kappa_w K_m'(\kappa_w)}\left(\frac{\omega R}{s_t}\right)^2 \tag{8}$$

describes the effect of water on the vibration of the filament. In the absence of water, $W=0$, Eqs. (6) and (7) reduce to these for elastic vibrations of a free cylindrical rod [38,40]. The dispersion relation of the vibrations in a water-filament system is obtained by requiring that the determinant of matrix $\mathcal{D}$ equals zero, and is analyzed in the following section.

III. ANALYSIS OF FILAMENT VIBRATIONS

The dispersion relation for the vibration of cylindrical rods specifies an infinite number of modes ω_{mj} for each m, which we numerate as $j=0,1,2,\ldots$. Below we analyze two distinct cases of axisymmetric ($m=0$) and flexural ($m\geqslant 1$) vibrations.

A. Axisymmetric vibrations

In the case of axisymmetric vibrations ($m=0$) the characteristic equation specified by the matrix $\mathcal{D}$ in Eq. (7) defines two uncoupled sets of modes corresponding to pure torsional and radial-longitudinal vibrations. The *torsional* vibrations of the filament [see Fig. 1(a)] are decoupled from the water motion and are characterized by the dispersion law

$$\omega_{0j}^{(t)}=s_t\sqrt{(\xi_j/R)^2+k_z^2} \tag{9}$$

and the displacement vector with components $u_r=u_z=0$,

$$u_\varphi\propto J_1(\xi_j r). \tag{10}$$

Here the integer index j numerates nonzero solutions of equation $J_2(\xi_j)=0$. In addition to the generic set of solutions in Eqs. (9) and (10), there exists a special mode $\omega_{00}^{(t)}$ with a linear dispersion law,

$$\omega_{00}^{(t)}=s_t k_z \tag{11}$$

and the displacement $u_\varphi\propto r^2$, which does not belong to a general solution of Eqs. (1) and (3) of the elastic equations of motion.

The *radial-longitudinal* modes [see Fig. 1(b)] are specified by a characteristic equation

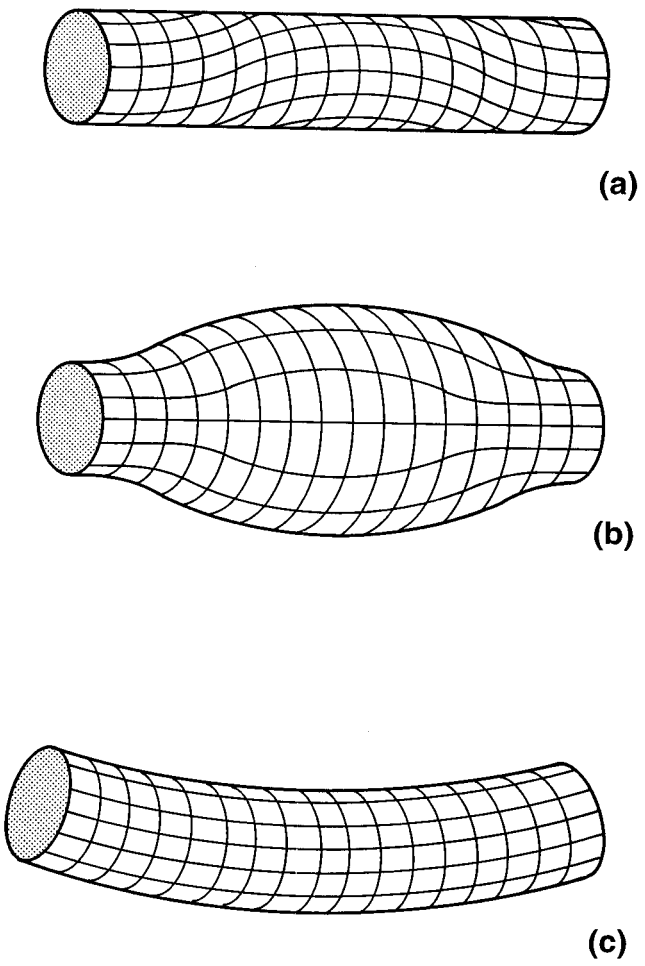

FIG. 1. Schematic view of displacement patterns for different vibrational modes of a filament: (a) axisymmetric torsional mode; (b) axisymmetric radial-longitudinal mode; (c) example of a flexural mode.

$$4k^2\kappa_t^2\frac{I_0(\kappa_t)}{\kappa_t I_1(\kappa_t)}=(k^2+\kappa_t^2)^2\frac{I_0(\kappa_l)}{\kappa_l I_1(\kappa_l)}+2(1+W)(k^2-\kappa_t^2), \tag{12}$$

where the filament-water coupling factor W is given by Eq. (8). Note that Eq. (12) is written in the assumption $\kappa_l^2>\kappa_t^2>0$, i.e., $\omega>s_t k_z$. If this condition does not hold, the modified Bessel's function I should be replaced by function J as shown in the Appendix.

In the absence of water, $W=0$, Eq. (12) is reduced to the Pochhammer equation and was analyzed in much detail [40]. The dispersion relation for the *lowest* radial-longitudinal mode $\omega_{00}^{(lr)}$ in the limits of small and large wave vectors k has the following behavior:

$$\omega_{00}^{(lr)}(k)\simeq\begin{cases}\sqrt{E/\rho}k_z, & k\ll 1,\\ s_{\mathrm{surf}}k_z z, & k\gg 1\,.\end{cases} \tag{13}$$

Thus, in the *long-wavelength* limit the acoustic mode $\omega_{00}^{(lr)}(k)$ corresponds to longitudinal waves in thin rods [38] with propagation speed of $\sqrt{E/\rho}$. Since the water-filament coupling term W given by Eq. (8) tends to zero at small frequencies ω, the asymptotic relation $\omega_{00}^{(lr)}(z)\simeq\sqrt{E/\rho}k$ is not changed in the presence of water. In the *short-wavelength* limit, this mode describes the surface (interface) Rayleigh (Stonley) wave propagating near cylinder surface (water-cylinder interface). Corresponding propagation speed s is found as a solution of standard algebraic equations for Rayleigh or Stonley velocities [38].

In the absence of water [40], the dispersion of *higher order* radial-longitudinal modes, $\omega_{0j}^{(lr)}(k_z)$ with $j\geqslant 1$, can be characterized by the following interpolation formula, valid in the limits of $k\ll 1$ and $k\gg j+1$:

$$\omega_{0j}^{(lr)}(k_z)\simeq s_t\sqrt{(\zeta_j/R)^2+k_z^2}, \tag{14}$$

where constants ζ_j are given by nonzero roots of the following two equations:

$$J_1(s_l\zeta_j/s_t)=0\,,\quad (s_l\zeta_j/2)J_0(\zeta_j)=J_1(\zeta_j). \tag{15}$$

In the intermediate region, $1\ll k\ll j+1$, the waves propagate with a bulk longitudinal sound speed, $\omega\propto s_l k_z$.

Thus, at $k=0$, the modes with $j\geqslant 1$ have finite cutoff frequencies equal to $\zeta_j R/s_t$. The situation is changed when water is present. When $W\neq 0$, the region $\omega>s_w k_z$ corresponds to radiation of acoustic waves out of the filament, and is characterized by a complex frequency spectrum. Analysis of Eq. (12) shows that, with a decrease of k_z, the branches $\omega_{0j}^{(lr)}$ enter the radiational sector $\omega>s_w k_z$ at frequencies ω_j, given by nonzero solutions of either of the following two equations:

$$J_1(\omega_j R\sqrt{s_w^{-2}-s_t^{-2}})=0\quad\text{or}\quad J_1(\omega_j R\sqrt{s_w^{-2}-s_l^{-2}})=0\,. \tag{16}$$

Finally, in the limit of large wave vector k_z, independent of the presence of water, the dispersion relation takes the form $\omega\simeq s_t k_z$, corresponding to the confined transverse waves in the filament.

B. Flexural waves

Vibrations with $m\geqslant 1$ describe the flexural waves of the filament, and are specified by Eqs. (6) and (7). It has been shown [26] that, in the absence of water, there exists only one flexural mode [see Fig. 1(c)], emanating from the origin [i.e., $\omega(0)=0$]. This branch corresponds to azimuthal number $m=1$ and is characterized by a parabolic dispersion at $k_z\ll 1$:

$$\omega_{10}(k_z)\simeq\sqrt{E/\rho}Rk_z^2/2. \tag{17}$$

Such a type of vibration corresponds to the bending mode of very thin rods and is predicted by a simple linear model [38]. Since the water-cylinder coupling term, defined by Eq. (8), vanishes at small ω and k_z, the long-wavelength asymptotics, given by Eq. (17), holds in the presence of water as well.

The rest of the flexural modes, in the absence of water, have finite cutoff frequencies at $k_z=0$. With water present, their frequencies gain a negative imaginary part at $\omega>s_w k_z$, and the acoustic energy is radiated from the wire. At large wave vector, $k_z\gg m+1$, all flexural modes behave

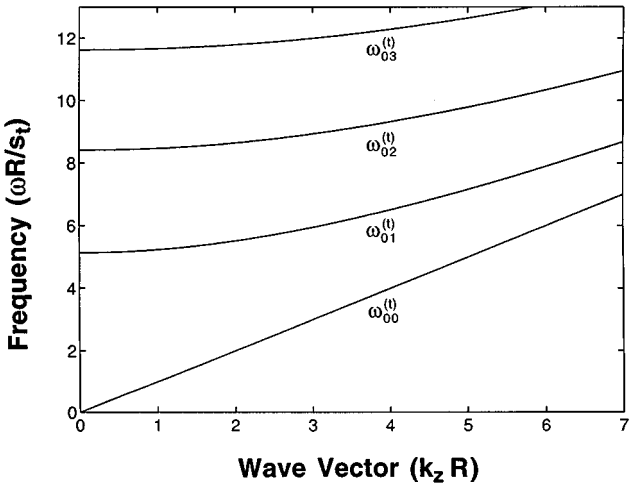

FIG. 2. Dimensionless frequency $\omega R/s_t$ vs dimensionless wave vector $k=Rk_z$ for axisymmetric $(m=0)$ *torsional* vibrations of a cylindrical filament.

like transverse waves, $\omega_{mj}\simeq s_t k_z$, while in the intermediate region of $1\ll k_z\ll m+1$ the dependence $\omega_{mj}\simeq s_l k_z$ is revealed.

IV. NUMERICAL RESULTS AND DISCUSSION

Analysis of Eqs. (6)–(8) performed in Sec. III provides a qualitative description of elastic filament vibrations in a water environment. In order to visualize the dispersion relations, we present the calculated dependence $\omega(k)$ for axisymmetric torsional and radial-longitudinal waves in Figs. 2 and 3, respectively. To emphasize the *universal* properties of filament vibration, independent of absolute values of radius R and material propagation speed s_t, we use the dimensionless frequency $\omega R/s_t$ and the dimensionless wave vector $k=k_z R$.

In Fig. 2 we present the dispersion relations for a set of axisymmetric *torsional* vibrations of a cylindrical filament. Since in our treatment the friction between water and filament surface is neglected, the pure torsional vibrations of the filament are not coupled with the water motion, and are essentially free. As seen from Fig. 2, there exists one acoustic torsional wave with a linear dispersion law and propagation speed s_t, given by Eq. (11). The higher torsional modes, given by Eq. (9), are characterized by finite cutoff frequencies at $k=0$, and phase velocities approaching s_t in the short-wavelength limit.

The spectrum of the *radial-longitudinal* vibrations, given by Eq. (12), is more complicated (see Fig. 3). The frequencies of the filament vibrations in the presence of water and without the surrounding water are marked by solid and dashed lines, respectively; the dotted straight lines correspond to $\omega=s_l k_z$ and $\omega=s_t k_z$. Even in the case of free filament vibrations, the form of modes depends on a dimensionless parameter $s_l/s_t=\sqrt{2(1-\nu)/(1-2\nu)}$. Since the absolute value of the Poisson's constant ν is unknown for most macromolecules, we choose a typical value of $\nu=0.3$, leading to the ratio of bulk longitudinal and transverse propagation speeds $s_l/s_t\approx 1.87$.

As seen from Fig. 3, the free vibrations of the filament (dashed lines) are characterized by one acoustic mode and a set of higher modes with finite cutoff frequencies. In the long-wavelength limit, the acoustic wave propagates with a speed $\sqrt{E/\rho}\approx 1.61 s_t$, in agreement with results of a simple linear theory; at large k the acoustic mode becomes a surface wave with a propagation speed equal to Rayleigh velocity, $s_{\mathrm{surf}}\approx 0.93 s_t$. The higher modes demonstrate an anticrossing behavior in the region $s_l k_z<\omega<s_t k_z$, and have a phase velocity approaching s_t at higher wave vector k_z.

When the vibrations of filament are considered in the presence of a water environment, the form of the dispersion law is characterized by two additional dimensionless constants: the ratio of water and the filament density, ρ_w/ρ, and the ratio of sound speed in water and in the filament, s_w/s_t. For concreteness, in Fig. 3 we presented the results of numerical calculations with parameters ρ_w/ρ and s_w/s_t, corresponding to that for AFs. We note that for AFs the limits of applicability of the continuous approach are limited rather severely by the inequality $k\lesssim 1$, since the effective radius of AF is of the order of that of an individual monomer. However, in the case of AF we can rely on the experimentally measured elastic constants and can compare qualitatively our results with normal-mode analysis by ben-Avraham and Tirion [37]. We also discuss below how the different values of the dimensionless parameters ρ_w/ρ and s_w/s_t change the dispersion relations depicted in Fig. 3.

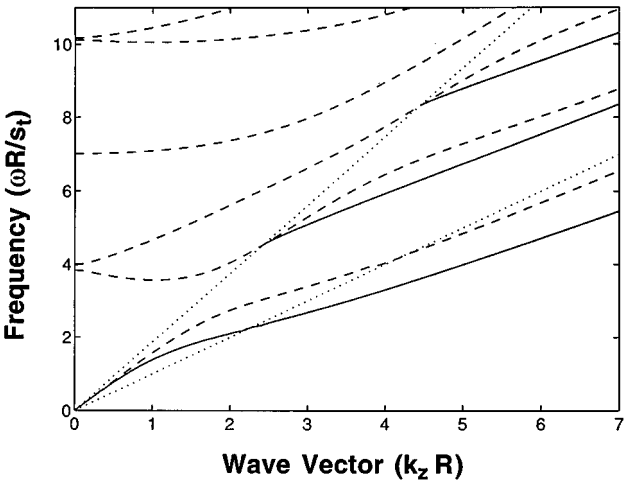

FIG. 3. Dispersion relations, $\omega_{0j}^{(lr)}(k)$, for axisymmetric *radial-longitudinal* vibrations of the cylindrical filament. Solid (dashed) lines correspond to vibrations of the filament with (without) water, and modes with $j=0,1,2$ $(j=0,\ldots,5)$. Dotted lines correspond to $\omega=s_l k_z=s_w k_z$ (upper line) and $\omega=s_t k_z$ (lower line). Other notations coincide with those in Fig. 2.

As for elastic constants, the experimentally measured quantity is ES, where S is an effective cross-section of a filament. Recent measurements of the parameter ES for AFs give the values of 43.7 ± 4.6 nN [15] and 46.8 ± 2.8 nN [17]. Using the value $ES=46$ nN, the mass of the actin monomer $M=43$ kDa, and the rise per monomer $\ell=2.75$ nm, we find the propagation speed of acoustic radial-longitudinal wave equal to $\sqrt{E/\rho}=\sqrt{ES\ell/M}\approx 1.3$ km/s. Then, using the

adopted value of Poisson's ratio, $\nu=0.3$, we find a transverse sound speed, $s_t=\sqrt{E/2(1+\nu)\rho}\approx 800$ m/s, and a longitudinal sound speed, $s_l=\sqrt{(1-\nu)E/(1-2\nu)(1+\nu)\rho}\approx 1.5$ km/s, of the AF material. The bulk longitudinal propagation speed s_l of AF material practically coincides with the sound speed in water, $s_l\approx s_w$. Finally, to find the AF radius R and density ρ, we should introduce a somewhat arbitrarily defined cross-section area S. Taking $S=25$ nm^2 [15], we obtain the radius $R=\sqrt{S/\pi}\approx 28$ Å and filament density $\rho=M/\ell S\approx 1.05$ g/cm^3. We also find that the dimensionless frequency, $\omega R/s_t$, of Figs. 1 and 2 corresponds to a cyclic frequency $f_0=s_t/2\pi R\approx 45$ GHz when $\omega R/s_t=1$.

The dispersion relations for the axisymmetric radial-longitudinal modes correspond to solid lines in Fig. 3. The most important effect of water on the vibration of the filament is that the acoustic energy is radiated by those waves with the phase velocities, ω/k_z, exceeding the speed of sound in water, s_w. The lowest (i.e., acoustic) mode has, in the long-wavelength limit, a propagation speed $\sqrt{E/\rho}\approx 1300$ m/s which is lower than the sound speed in water, and is not affected by the presence of solvent for $k\ll 1$. At large wave vector k, the lowest mode corresponds to interface vibrations and has a propagation speed $s_{\rm surf}$, lower than the Rayleigh speed in the absence of water. In the region $\omega>s_w k_z$, the higher-order modes are radiated from the filament and are not shown in Fig. 3, since their frequencies are complex. The frequencies of the higher-order modes coincide with those for a free filament at $\omega=s_w k_z$, and in the region of $\omega>s_w k_z$ the vibrational frequencies in the coupled water-filament system are slightly lower than those for a free filament. At large wave vector, $k_z>\omega/s_t$, the propagation speeds for waves in both filament-water system and free filament approach the bulk transverse speed s_t. We do not present the numerical results for the flexural modes ($m\geqslant 1$), since qualitatively the behavior of these modes is similar to higher-order modes in Fig. 3. The only exception occurs in the case of $m=1$, where an additional bending mode arises [26] with the parabolic dispersion law, given by Eq. (17).

For the case of comparatively thin AFs, the theory developed herein is near the limit of its applicability; however, it is interesting to compare Figs. 2 and 3 with the results of the normal-modes study of AFs by ben-Avraham and Tirion [37]. These authors solved quasiperiodic equations of motion for rigid actin monomers forming a helical structure. Taking six degrees of freedom per each monomer, the authors of Ref. [37] calculated the frequencies of six vibrational modes as a function of the phase lag ϕ between the monomers. It is important to note that due to higher (cylindrical) symmetry of the filament in our phenomenological model, the normal modes are characterized by wave vector k_z (due to the translational invariance) and an azimuthal number m (due to the rotational symmetry). In a more realistic helical model, there exist no pure translational or rotational symmetries, but instead only the symmetry of simultaneous translational-rotational transformation described by the helical number ϕ. The correspondence between the cylindrical numbers k_z, m, and the helical number ϕ is established by the relation

$$\phi=k_z\ell+m\phi_0, \tag{18}$$

where $\ell=2.75$ nm is the rise per monomer and $\phi_0=166.15°$ is the angle of rotation between subsequent monomers.

Combining, with the help of Eq. (18), Figs. 2 and 3 for axisymmetric vibrations as well as modes with $m\geqslant 1$, we obtain the dispersion dependence which is qualitatively similar to that of Ref. [37], for wave vector $|k|<1$. Both approaches reproduce two acoustic modes (at $\phi\ll 1$, or $k\ll 1$ and $m=0$) and one helical mode (at $\phi\approx\phi_0$, or $k\ll 1$ and $m=1$) predicted by the simple linear model, as well as the finite cutoff frequencies of higher modes in the absence of water, and complex anticrossing behavior along the line with $\omega=s_l k_z$. There also exist several dissimilarities due to the differences in the models. The continuous model is unable to describe the dispersion law in the region of $\phi\approx\pi/2$, while the *ad hoc* calculations provide important information on merging of different modes. The normal mode analysis, based on the assumption of *rigid* monomers, resulted in only six branches; inclusion of the internal degrees of freedom would lead to a larger number of vibrational modes, in qualitative agreement with the elastic continuum model. The microscopic calculations of ben-Avraham and Tirion, based on a single fitting parameter, resulted in the propagation speed $s_t=410$ m/s for the torsional vibrations. This value, compared to the speed $\sqrt{E/\rho}\approx 1.3$ km/s of radial-longitudinal vibrations (reproduced in both models), results in an unphysical value of Poisson's ratio, $\nu\approx -3.5$, and therefore contradicts the assumption of isotropic elastic continuum. At last, our treatment provides information about the effects of solvent on the AF vibration, with the most important conclusion being that the acoustic energy is radiated from AF over wide ranges of frequency and wavelength.

Finally, we discuss how the dispersion law, depicted in Fig. 3 for the specific values $\rho_w/\rho=0.95$ and $s_w=1.88 s_t$, varies as parameters change. It follows from Fig. 3 that the form of dispersion curves for the water-filament vibrations (solid lines) can be qualitatively predicted from the dispersion law for waves in a free filament (dashed lines). As follows from the above analysis, the line $\omega=s_w k_z$ separates the regions of water-filament vibrations, localized in the vicinity of the filament from the regime of acoustic energy radiation. Therefore, the dispersion curves for free filament waves should be cut to the right of the $\omega=s_w k_z$ line. Second, the coupling parameter ρ_w/ρ specifies how much the frequencies in water-filament system deviate from the frequencies of a free filament vibration. In no case can the dispersion curves for a coupled system touch or cross the dispersion curve for a free filament, corresponding to another (lower) vibrational mode. Thus, Figs. 2 and 3 provide qualitative information on the *universal* properties of the vibrational spectrum for an arbitrary cylindrical filamentous macromolecule.

V. CONCLUSION

In contrast to the motion of globular proteins, which is characterized by confined vibrational modes, long filamentous macromolecules support the *propagation* of elastic waves. Thus, it is convenient to describe the dynamics of long proteins as a superposition of mechanical waves with different frequencies ω and wave vectors k along the macromolecule. The most fundamental properties of the protein

motion can be deduced from the dispersion law of these modes and the pattern of vibration for each individual mode.

In this paper we described the general, universal properties of long protein dynamics by treating the protein as a continuous medium and using the formalism of classical elasticity theory. While this model does not provide detailed information about microscopic movements of each constituent element, such an approach can describe adequately the most important long-range, collective conformal motion of the protein. The relative simplicity of the results thus obtained, their independence on specific structure of the protein, emphasis on the most universal properties of vibrations, and the inclusion of the solvent effects in the natural way allow this approach to complement *ad hoc* microscopic study of protein dynamics.

As specific implementations of our model (see also [19]), we have chosen two types of structures: long cylindrical rods (present paper) and hollow cylindrical shells [19] filled with a solvent. These two topologically different geometries serve as physically reasonable approximations for a large variety of filamentous structures, such as MTs, AFs, and IFs. The elastic parameters of the model have been taken from measurements of flexural rigidity of these objects. The waves propagating near the shell (filament) interface were classified and characterized according to their pattern, and the dispersion of these waves was analyzed both analytically and numerically. In the long-wavelength limit, the results of the simple linear theory for thin elastic rods have been reproduced.

In particular, for cylindrical geometry (filaments), two acoustic waves and one helical wave have been found. As for water-shell system (microtubules), there exist three acoustic modes (one of them appears due to interaction with solvent) and a set of helical, flexural waves [19]. Both structures also support higher frequency waves which become radiative at large wavelength with mechanical energy leaking to the surrounding solvent. The results obtained in this paper are of general, universal character and complement detailed microscopic calculations of long protein dynamics.

ACKNOWLEDGMENTS

This study was supported in part, by the U.S. Army Research Office and the Office of Naval Research. The authors also acknowledge many helpful discussions with Dr. Oksana Sirenko on biological aspects of this work.

APPENDIX

In Eq. (3) for scalar potentials in a filament-water system, we have chosen the solutions of the wave equation in the *inner* part of the filament in terms of the modified Bessel's function I. These solutions describe interface vibrations, decaying exponentially toward the center of the MT or filament, and correspond to the case of $\kappa_l^2, \kappa_t^2 > 0$. The opposite case corresponds to confined vibrations, involving the whole interior part of the filament. Such vibrations can be still described by the same equations after replacement of modified Bessel's functions I by Bessel's functions J according to the identity

$$I_m(-i|\kappa|) = i^{-m} J_m(|\kappa|). \tag{A1}$$

As for the *outer* region, we have chosen the solutions in terms of exponentially decreasing MacDonald's functions K. Thus, the scalar potentials in the outer region, described by Eq. (3), correspond to evanescent waves in the surrounding water, provided that $\kappa_w^2 > 0$. In the opposite case of $\omega > s_w k_z$, the acoustic energy is radiated from the MT or filament, and the system is characterized by a frequency spectrum with a negative imaginary part. The scalar potential takes the form of outgoing cylindrical waves, and can be treated with the help of the identity

$$K_m(-i|\kappa|) = (\pi/2) i^{m+1} H_m^{(1)}(|\kappa|), \tag{A2}$$

where $H_m^{(1)}$ is a Hankel's function of the first kind.

[1] K. Sekimoto *et al.*, Phys. Rev. Lett. **75**, 172 (1995).
[2] L. Bordieu *et al.*, Phys. Rev. Lett. **75**, 176 (1995).
[3] K. Sekimoto and K. Tawada, Phys. Rev. Lett. **75**, 180 (1995).
[4] S. Iijima, Nature (London) **354**, 56 (1991); S. Iijima and T. Ichihashi, *ibid.* **363**, 603 (1993); T.F. Nagy *et al.*, Phys. Rev. B **50**, 12 208 (1994); P.V. Huong *et al.*, *ibid.* **51**, 10 048 (1995).
[5] A.K. Viswanath *et al.*, Microw. Opt. Tech. Lett. **7**, 94 (1994); P.M. Campbell *et al.*, Solid-State Electron **37**, 583 (1994); K. Yoh *et al.*, Semicond. Sci. Technol. **9**, 961 (1994).
[6] K. Luby-Phelps, Curr. Opinion Cell Biol. **6**, 3 (1994).
[7] D. Bray, *Cell Movements* (Garland, New York, 1992).
[8] R.D. Vale, Annu. Rev. Cell Biol. **3**, 347 (1987).
[9] L.A. Amos and W.B. Amos, *Molecules of Cytoskeleton* (Guilford, New York, 1991).
[10] L. Beese, G. Stubbs, and C. Cohen, J. Mol. Biol. **194**, 257 (1987); D. Chrétien and R.H. Wade, Biol. Cell. **71**, 161 (1991).
[11] K.C. Holmes *et al.*, Nature (London) **347**, 44 (1991); M. Lorenz, D. Popp, and K.C. Holmes, J. Mol. Biol. **234**, 826 (1993).
[12] M. Stewart, Curr. Opinion Cell. Biol. **2**, 91 (1990).
[13] J. Mizushima-Sugano *et al.*, Biochem. Biophys. Acta. **755**, 257 (1983).
[14] H. Nagashima and S. Asakura, J. Mol. Biol. **136**, 169 (1980); T.M. Yanagida *et al.*, Nature (London) **307**, 58 (1984).
[15] F. Gittes *et al.*, J. Cell. Biol. **120**, 923 (1993).
[16] P. Venier *et al.*, J. Biol. Chem. **269**, 13 353 (1994).
[17] H. Kojima, A. Ishijima, and T. Yanagida, Proc. Natl. Acad. Sci. **91**, 12 962 (1994).
[18] H.E. Huxley *et al.*, Biophys. J. **67**, 2411 (1994); K. Wakabayashi *et al.*, *ibid.* **76**, 2422 (1994).
[19] Yu.M. Sirenko, M.A. Stroscio, and K.W. Kim, Phys. Rev. E **53**, 1003 (1996).
[20] J.A. McCammon and S.C. Harvey, *Dynamics of Protein and Nucleic Acids* (Cambridge University Press, Cambridge, England, 1978).
[21] H. Fraunfelder, F. Parak, and R.D. Young, Ann. Rev. Biophys. Biophys. Chem. **17**, 451 (1988).

[22] E.L. Beer *et al.*, Biophys. J. **68**, 70s (1995).
[23] C.R. Bagshaw, *Muscle Contraction* (Chapman and Hall, New York, 1993).
[24] D.A. Winkelmann *et al.*, Biophysical J. **68**, 2444 (1995); K. Saito *et al.*, *ibid.* **66**, 769 (1994); J.T. Finner, R.M. Simmons, and J.A. Spudich, Nature (London) **368**, 113 (1994).
[25] M.M. Magnasco, Phys. Rev. Lett. **71**, 1477 (1993); **72**, 2656 (1994).
[26] V.G. Grigoryan and D.G. Sedrakyan, Akust. Zh. **29**, 470 (1983) [Sov. Phys. Acoust. **29**, 281 (1984)].
[27] M.A. Stroscio *et al.*, J. Appl. Phys. **76**, 4670 (1994); M.A. Stroscio and K.W. Kim, Phys. Rev. B **48** 1936 (1993); S. Yu *et al.*, *ibid.* **50**, 1733 (1994); **51**, 4695 (1995).
[28] N. Nishiguchi, Jpn. J. Appl. Phys. **33**, 285 (1994); Phys. Rev. B **50**, 10 970 (1994); **52**, 5279 (1995); M.A. Stroscio *et al.*, J. Phys. Condens. Matter **8**, 2143 (1996).
[29] M.V. Satarić, J.A. Tuszyński, and R.B. Žakula, Phys. Rev. E **48**, 589 (1993).
[30] E.C. Lin and H.F. Cantiello, Biophys. J. **65**, 1371 (1993).
[31] C.F. Schmidt *et al.*, Macromolecules **22**, 3637 (1989); D.H. Boal, Biophys. J. **67**, 521 (1994); K.S. Zaner, *ibid.* **68**, 1019 (1995).
[32] M. Levitt, C. Sander, and P.S. Stern, J. Mol. Biol. **181**, 423 (1985).
[33] D. ben-Avraham, Phys. Rev. B **47**, 14 559 (1993).
[34] M.M. Tirion and D. ben-Avraham, J. Mol. Biol. **230**, 186 (1993).
[35] W. Kabsch *et al.*, Nature (London) **347**, 37 (1990).
[36] M.M. Tirion, D. ben-Avraham, and K.C. Holmes, in *Actin: Biophysics, Biochemistry, and Cell Biology*, edited by J.E. Estes and P.J. Higgins (Plenum, New York, 1994), pp. 3–12; M.M. Tirion *et al.*, Biophys. J. **68**, 5 (1995).
[37] D. ben-Avraham and M.M. Tirion, Biophys. J. **68**, 1231 (1995).
[38] K.F. Graff, *Wave Motion in Elastic Solids* (Clarendon, Oxford, 1975).
[39] A.P. Demchenko, O.I. Rusyn, A.M. Egorov, and V.I. Tishkov, Biochem. Biophys. Acta **1039**, 290 (1990).
[40] M. Onoe, H.D. McNiven, and R.D. Mindlin, J. Appl. Mech. **29**, 729 (1962).